NRL Memorandum Report 3768

High Frequency Drift Waves with Wavelengths Below the Ion Gyroradius in Equatorial Spread F

J. D. Huba, P. K. Chaturvedi and S. L. Ossakow

Plasma Physics Division

and

D. M. Towle

MIT Lincoln Laboratory
Lexington, Massachusetts 02173

May 1978

This research was sponsored in part by the Office of Naval Research, and by the Defense Nuclear Agency under subtask I25AAXYX960, work unit code 11 and work unit title "WB Scintillation Assessment."

NAVAL RESEARCH LABORATORY
Washington, D.C.

SECURITY CLASSIFICATION OF THIS PAGE (When Data Entered)

REPORT DOCUMENTATION PAGE

READ INSTRUCTIONS BEFORE COMPLETING FORM

1. REPORT NUMBER: NRL Memorandum Report 3768

2. GOVT ACCESSION NO.:

3. RECIPIENT'S CATALOG NUMBER:

4. TITLE (and Subtitle): HIGH FREQUENCY DRIFT WAVES WITH WAVELENGTHS BELOW THE ION GYRORADIUS IN EQUATORIAL SPREAD F

5. TYPE OF REPORT & PERIOD COVERED: Interim report on a continuing NRL problem.

6. PERFORMING ORG. REPORT NUMBER:

7. AUTHOR(s): J. D. Huba*, P. K. Chaturvedi**, S. L. Ossakow, and D. M. Towle†

8. CONTRACT OR GRANT NUMBER(s):

9. PERFORMING ORGANIZATION NAME AND ADDRESS: Naval Research Laboratory, Washington, D. C. 20375

10. PROGRAM ELEMENT, PROJECT, TASK AREA & WORK UNIT NUMBERS: NRL Problem A03-16B and H02-42D; DNA Subtask I25AAXYX960

11. CONTROLLING OFFICE NAME AND ADDRESS: Defense Nuclear Agency, Washington, D.C. 20305 and Office of Naval Research, Arlington, Virginia 22217

12. REPORT DATE: May 1978

13. NUMBER OF PAGES: 34

14. MONITORING AGENCY NAME & ADDRESS (if different from Controlling Office):

15. SECURITY CLASS. (of this report): UNCLASSIFIED

15a. DECLASSIFICATION/DOWNGRADING SCHEDULE:

16. DISTRIBUTION STATEMENT (of this Report): Approved for public release; distribution unlimited.

17. DISTRIBUTION STATEMENT (of the abstract entered in Block 20, if different from Report):

18. SUPPLEMENTARY NOTES: This research was sponsored in part by the Office of Naval Research and by the Defense Nuclear Agency under subtask I25AAXYX960, work unit code 11 and work unit title "WB Scintillation Assessment."

(Continues)

19. KEY WORDS (Continue on reverse side if necessary and identify by block number)

Drift waves
F region irregularities
Near and below ion gyroradius
Linear theory
Equatorial Spread F
ALTAIR VHF and UHF radar

20. ABSTRACT (Continue on reverse side if necessary and identify by block number)

Evidence is given for intense VHF and UHF radar backscatter during equatorial Spread F resulting from irregularities of 1 meter and 36 cm, respectively. The linear theory for high frequency ($\omega \gtrsim \Omega_i$, where Ω_i is the ion gyrofrequency) drift waves, generated by the drift-cyclotron and lower-hybrid-drift instabilities, is presented. This linear theory is set forth as a possible explanation for the occurrence of these irregularities below the ion gyroradius. The maximum growth for these instabilities occurs for $kr_e \sim 1$, where k is the wavenumber perpendicular to the magnetic field and r_e is the electron gyroradius. For these instabilities,

(Continues)

DD FORM 1 JAN 73 1473 EDITION OF 1 NOV 65 IS OBSOLETE
S/N 0102-014-6601

SECURITY CLASSIFICATION OF THIS PAGE (When Data Entered)

18. Supplementary Notes (Continues)

*Science Applications Inc., McLean, Virginia 22101
**University of Maryland, College Park, Maryland 20742
†MIT Lincoln Laboratory, Lexington, Massachusetts 02173

20. Abstract (Continued)

the growth rate is $\gamma \gtrsim (m_e/m_i)^{1/4}\Omega_i$ and results in growth times less than a second. For typical equatorial Spread F ionospheric parameters, where $(\nu_{ii}/\Omega_i)\,(kr_i)^2 \gtrsim 1$ (ν_{ii} is the ion-ion collision frequency, r_i is the ion gyroradius), the lower-hybrid-drift instability is dominant.

HIGH FREQUENCY DRIFT WAVES WITH WAVELENGTHS BELOW THE ION GYRORADIUS IN EQUATORIAL SPREAD F

I. Introduction

Recently in August 1977, during a coordinated ground based measurement campaign conducted at Kwajalein in the Marshall Islands, under the auspices of the Defense Nuclear Agency, the ALTAIR radar (operated by MIT Lincoln Laboratory) observed enhanced backscatter from equatorial Spread F at 155 MHz and 415 MHz (see Fig. 1; a detailed description of these radar measurements will appear in another paper). This corresponds to F region irregularities at ~ 1 m and ~ 36 cm, respectively, which are below the O^+ gyroradius. Since these irregularities correspond to $kr_i \gg 1$ they cannot be explained by the linear theory of the universal drift instability (Kadomtsev, 1965; Costa and Kelley, 1978 a,b). In the present letter we suggest that the drift-cyclotron instability (DC) (Mikhailovskii and Timofeev, 1963) or the lower-hybrid-drift instability (LHD) (Krall and Liewer, 1971) can account for small scale F region irregularities. These instabilities are excited by sharp density gradients which presumably evolve nonlinearly from a long wavelength Rayleigh-Taylor instability (i.e., a two step process; see Haerendel, 1974 and Hudson et al., 1973). In fact, Costa and Kelley (1978a) have presented in situ rocket data showing the existence of density gradients with scale lengths ⩾ 25 meters.

In a collisional plasma, i.e., the equatorial Spread F ionosphere, the parameter which predominately determines which instability (DC or LHD) will be excited is

$$C_f = (\nu_{ii}/\Omega_i)k^2r_i^2$$

Note: Manuscript submitted March 23, 1978.

where ν_{ii} is the ion-ion collision frequency, Ω_i is the ion gyrofrequency, r_i is the ion gyroradius, and k is the wavenumber perpendicular to the magnetic field. We note that C_f corresponds to ion viscosity in a fluid theory. The DC instability can be excited in a dense plasma ($\omega_{pe}^2 \gg \Omega_e^2$, where ω_{pe} is the electron plasma frequency and Ω_e is the electron gyrofrequency) when

$$L/r_i < (1/2\ell)\ (m_i/2m_e)^{\frac{1}{2}} \text{ and } C_f \ll 1$$

with a real frequency and growth rate given by $\omega_r \approx \ell\Omega_i$ and $\gamma \approx (m_e/m_i)^{\frac{1}{4}}\ \ell\Omega_i$, respectively (Mikhailovskii and Timofeev, 1963). Here L is the plasma inhomogeneity (density gradient) scale length, ℓ is the cyclotron harmonic excited, and m_e and m_i are the masses of the electron and ion, respectively. For O^+ ($m_i = 16\ H^+$), T = 1000 °K where r_i = 5.6 m (typical F region parameters), the above condition on L corresponds to L < 340 m (for the first harmonic, $\ell = 1$). Maximum growth occurs for $kr_e \approx (2T_e/T_i)^{\frac{1}{2}} \approx 1$ (for the F region ionosphere) where r_e is the electron gyroradius. For $kr_e \approx 1$ (i.e., $kr_i \approx 170$) the condition $C_f \ll 1$ becomes $\nu_{ii}/\Omega_i \ll m_e/m_i$, which for typical F region parameters corresponds to $n \ll 10^3$ (n is electron density in units of cm^{-3}). More generally the condition on C_f for DC is, for typical F region parameters, $(kr_i)^2\ n \ll 2 \times 10^7$, so that for somewhat longer wavelengths the condition on density becomes less restrictive.

On the other hand, if $C_f \gtrsim 1$ the ion-ion collisions destroy the ion gyroresonances, necessary for the DC instability, (Dougherty, 1964;

Allan and Sanderson 1976) and the DC instability transforms into the LHD instability even though $\nu_{ii} \ll \Omega_i$. The LHD instability is characterized by

$$\frac{\omega_r}{\Omega_i} \sim \frac{r_i}{L}\left(\frac{m_i}{m_e}\right)^{\frac{1}{2}}, \quad \frac{\gamma}{\Omega_i} \sim \left(\frac{r_i}{L}\right)^2\left(\frac{m_i}{m_e}\right)^{\frac{1}{2}}$$

where the angular frequency $\omega \equiv \omega_r + i\gamma$ and maximum growth occurs for $kr_e \sim (2T_e/T_i)^{\frac{1}{2}} \sim 1$ (Davidson et al., 1977). In the collisionless limit, the DC instability transforms into the LHD instability for $L/r_i \leqslant (m_i/m_e)^{\frac{1}{4}}$. For typical ionospheric parameters this corresponds to $L \leqslant 30$m, which occurs infrequently (Costa and Kelley, 1978a). However, in the $C_f \geqslant 1$ collisional regime for the LHD instability there is no threshold requirement on L.

Thus, these instabilities can produce small scale irregularities on very short time scales, which is consistent with previous observational evidence (Farley et al., 1970; Woodman and LaHoz, 1976) as well as in the ALTAIR data cited here. It should be pointed out that in this letter we are presenting two extreme regimes, viz., $C_f \ll 1$ and $C_f \geqslant 1$. In some instances (i.e., for certain densities, etc.) irregularity wavelengths ~ 1 m could fall in the regime $C_f \leqslant 1$. This transition regime (in C_f space) involves a more complicated analysis than is presented here and will be the subject of a future, more lengthy paper.

II. Linear Theory

Here we present a concise overview of the linear theory and its application to the equatorial Spread F ionosphere. A more detailed analysis will be presented in a later paper. We assume: (1) the plasma to be composed of electrons and O^+ ions, (2) the magnetic field to be constant and in the z direction ($\underline{B} = B_o\hat{z}$), and (3) the plasma density to depend on x only, $n_o = n_o(x)$. This density inhomogeneity produces a diamagnetic drift current such that $\underline{V}_d = (V_{di} - V_{de})\hat{y}$, where $V_{di} = (V_i^2/2\Omega_i)(\partial \ell n\ n_o/\partial x)$ and $V_{de} = -(V_e^2/2\Omega_e)(\partial \ell n\ n_o/\partial x)$ and V_i and V_e are the ion and electron thermal velocities, respectively. Here we are only interested in flute modes ($\underline{k}\cdot\underline{B} = 0$) and take perturbations of the form $\exp[i(ky-\omega t)]$, i.e., $\underline{k} = k\hat{y}$ ($\omega \equiv \omega_r + i\gamma$), which maximizes the linear growth (Gladd, 1976; Gary and Sanderson, 1977). The electrostatic approximation is made since $\beta \ll 1$ for the F region and use is made of the local approximation $kL \gg 1$, where $L^{-1} = \partial \ell n\ n_o/\partial x$.

The general dispersion relation describing the DC and the LHD instability is

$$D(\omega,k) = 1 + \chi_i + \chi_e = 0 \tag{1}$$

where

$$\chi_i = 2\left(\frac{\omega_{pi}}{kV_i}\right)^2 \left[1 + i\,\frac{\omega - kV_{di}}{\Omega_i}\,G_i\right] \tag{2}$$

$$\chi_e = 2\left(\frac{\omega_{pe}}{kV_e}\right)^2 \left[1 - \frac{\omega - kV_{de}}{\omega}\,\Gamma_o(b_e)\right] \tag{3}$$

$\Gamma_o(b_e) = e^{-b_e} I_o(b_e)$, $\omega_{p\alpha} = (4\pi n e^2/m_\alpha)^{\frac{1}{2}}$, $V_\alpha = (2T_\alpha/m_\alpha)^{\frac{1}{2}}$, $b_\alpha = (kr_\alpha)^2/2$, $r_\alpha = V_\alpha/\Omega_\alpha$, $\Omega_\alpha = eB/m_\alpha c$ and I_o is the modified Bessel function. For the DC instability, $C_f \ll 1$, (Freidberg and Gerwin, 1977; Gary and Sanderson, 1977)

$$G_i = \int_0^\infty dt\, \exp\left[i\omega t + b_i(\cos t - 1) - i\,\frac{kV_{di}}{\Omega_i}\sin t\right] \tag{4}$$

and for the LHD instability, $C_f \gtrsim 1$, (Allan and Sanderson, 1976)

$$G_i = -i \frac{\Omega_i}{kV_i} Z\left(\frac{\omega - kV_{di}}{kV_i}\right) \tag{5}$$

In order to better understand the physical nature of these instabilities, we will briefly consider the limit $T_e \to 0$, which results in a simple analytic dispersion relation. A numerical study of Eq. (1) for realistic F region parameters ($T_e \neq 0$) will be given afterward.

A. Drift-Cyclotron Instability. We assume $\omega \approx \ell\Omega_i$ (here $\ell = 1, 2\ldots$) and $b_i \gg 1$ and find that

$$D(\omega,k) = \frac{1}{2}\left(\frac{kV_i}{\omega_{pi}}\right)^2\left(1 + \frac{\omega_{pe}^2}{\Omega_e^2}\right) + \frac{\omega - kV_{di}}{\omega}\left(1 - \frac{\omega}{\omega - \ell\Omega_i}\Gamma_\ell(b_i)\right) = 0 \tag{6}$$

where $\Gamma_\ell(b_i) = I_\ell(b_i)\exp[-b_i]$. From Eq. (6) one can show that instability occurs for $V_{di}/V_i > (2m_e/m_i)^{\frac{1}{2}}\ell$ with a maximum growth rate $\gamma \approx \ell\Omega_i(m_e/m_i)^{\frac{1}{4}}$. The instability is reactive and is produced by the coupling of a drift wave ($\omega_1 \approx kV_{di}$) and an ion cyclotron wave ($\omega_2 \approx \ell\Omega_i$), which is clear from Eq. (6).

B. Lower-Hybrid-Drift Instability. For a sufficiently large ion-ion collision frequency ($C_f \gtrsim 1$) or drift velocity $V_{di}/V_i > (m_e/m_i)^{\frac{1}{4}}$ the DC instability makes a transition to the lower-hybrid-drift instability. Then the nature of the instability changes from reactive to dissipative. Physically, the ions behave as unmagnetized particles and can be resonant with a drift wave propagating perpendicular to $\underline{B}$. The dispersion equation for this instability is

$$D(\omega,k) = 1 + \frac{\omega_{pe}^2}{\Omega_e^2} + \frac{2\omega_{pi}^2}{k^2V_i^2}\left(1 - \frac{kV_{di}}{\omega} + i\sqrt{\pi}\,\frac{\omega - kV_{di}}{kV_i}\right) = 0 \tag{7}$$

which has the solution

$$\omega_r = kV_{di} \frac{2\omega_{pi}^2}{k^2V_i^2} \left(1 + \frac{2\omega_{pi}^2}{k^2V_i^2} + \frac{\omega_{pe}^2}{\Omega_e^2}\right)^{-1} \qquad (8)$$

$$\gamma = -\sqrt{\pi}\, \frac{\omega_r - kV_{di}}{kV_i} \, \frac{\omega_r^2}{kV_i} \qquad (9)$$

where we have assumed $\omega/kV_i \ll 1$. From Eq. (9) one finds instability for $\omega - kV_{di} < 0$.

For parameters typical of the equatorial Spread F region, we now solve Eq. (1) numerically to determine the nature of the unstable waves. Fig. 2 is a plot of γ/Ω_i vs kr_e for $V_{di}/V_i = 0.037$, $T_e = T_i$ and $\omega_{pe}/\Omega_e = 10$ (for $n = 10^6$ cm^{-3} and $B = 0.3$ gauss). For O^+ and $T_i = 1000^\circ K$, this V_{di}/V_i corresponds to $L \approx 13 r_i \approx 75$ meters, which is well within the range shown by Costa and Kelley (1978a), and also corresponds to $V_{di} \sim 40$ m/sec, which is well within the realm of bubble rise velocities exhibited by in situ measurements (Kelley et al., 1976; McClure et al., 1977) and numerical simulations (Ossakow et al., 1978). The solid curve corresponds to the DC instability (Eq. (4)) and the dashed curve corresponds to the LHD instability (Eq. (5)). We emphasize that the values of ν_{ii} and kr_i will determine which mode is excited. However, for most equatorial Spread F ionospheric parameters, the LHD or the transition region ($C_f \lesssim 1$) will be favored. Also, there are unstable waves for $kr_e \gg 1$ which are not shown in Fig. 2. Two important features of Fig. 2 are: (1) the maximum growth rate γ_M is a significant fraction of the ion cyclotron frequency ($\gamma_M \approx 0.17\Omega_i$ for DC and $\gamma_M = 0.08\Omega_i$ for LHD); and (2) unstable waves exist in the regime

$kr_i \gg 1$ ($kr_i \gtrsim 25$ or $kr_e \gtrsim 0.15$). If $C_f \ll 1$ the DC is excited with the $\ell \approx 1$ peak at $kr_e \approx 0.15$ corresponding to a wavelength $\lambda \sim 1$ meter and the $\ell = 3$ peak, extending to $kr_e \approx 0.58$, corresponding to $\lambda \approx 36$ cm (415 MHz backscatter). The LHD instability ($C_f \gtrsim 1$) has a continuous spectrum and can excite a broad range of wavelengths ($\lambda \sim$ 10cm - 2m).

Figure 3 is a plot of γ_M/Ω_i vs V_{di}/V_i for $T_e = T_i$ and $\omega_{pe}/\Omega_e = 10$, where γ_M is the maximum growth rate with respect to k. Again the solid curve is the DC instability and the dashed curve is the LHD instability. Note that the DC instability makes a transition to the LHD instability for $V_{di}/V_i \approx 0.11$. The essential features of this curve are that these instabilities can be excited at very low drift velocities ($V_d/V_i \approx 0.01$) and for moderate drifts ($V_{di}/V_i \approx 0.1$) can have very large growth rates ($\gamma \sim 0.6\ \Omega_i$).

III. Discussion and Summary

We have shown that the lower-hybrid-drift instability (LHD) or the drift-cyclotron (DC) instability can be active in the equatorial Spread F ionosphere. The parameter which predominately determines which instability will be excited is $C_f = (\nu_{ii}/\Omega_i)(kr_i)^2$. If $C_f \ll 1$, the DC instability can be unstable for $L/r_i < (m_i/8m_e)^{\frac{1}{2}}$. For O^+ ($m_i = 16\ H^+$), $T = 1000^0$K where $r_i \approx 5.6$ m, this corresponds to density gradient scale lengths $L < 340$ m which exist during equatorial Spread F conditions (Costs and Kelley, 1978a). The growth rate of the instability maximizes for $kr_e \approx 1$ and from the C_f condition this requires $\nu_{ii}/\Omega_i \ll m_e/m_i) \sim 3.4\mathrm{x}10^{-5}$ or $n \ll 10^3\ \mathrm{cm}^{-3}$. However, for longer unstable wavelengths such as $kr_i \approx 30$ ($\lambda \sim 1$m) the condition becomes $n \ll 2\mathrm{x}10^4 \mathrm{cm}^{-3}$.

This may be the case in the lower equatorial F region or well within equatorial Spread F bubbles. On the other hand, for $C_f \gtrsim 1$ the LHD instability can become unstable for which there is no threshold density gradient scale length. Since $C_f \gtrsim 1$ for most typical equatorial Spread F ionospheric parameters, we expect the LHD instability to be dominant.

Furthermore, these instabilities have very large growth rates ($\gamma \lesssim \Omega_i$) which result in growth times $\tau = \gamma^{-1}$ less than a second. This can account for the apparent rapid growth of the small scale irregularities observed by Jicamarca radar backscatter (Farley et al., 1970; Woodman and LaHoz, 1976) as well as by the ALTAIR radar. Since maximum growth occurs for $kr_e \approx 1$, taking $r_e = 3.3$ cm, we have that this corresponds to fluctuations with $\lambda \approx 21$ cm and this can account for the UHF (415 MHz) radar backscatter (see Fig. 1). Also, from the example given in Fig. 2, we note that unstable waves grow for $kr_e \approx 0.15$ which corresponds to irregularities with $\lambda \sim 1$m and this can explain the VHF (50 MHz and 155 MHz) radar irregularities. Thus, the DC or LHD instability can linearly excite the small scale irregularities observed by radar backscatter in the equatorial Spread F region on very short time scales.

We finally mention several points related to the excitation of these high frequency drift waves. First, although wavenumbers parallel to the magnetic field have not been considered in this letter ($k_{\parallel} = 0$), $k_{\parallel} \neq 0$ modes also exist with weaker growth rates (Gary and Sanderson, 1977). These waves, with finite $k_{\parallel}$, could account for the large wings observed in the Doppler spectra (as originally pointed out by Woodman and LaHoz, 1976). Second, the anomalous transport properties associated with the DC and LHD instabilities can be effective in limiting the amplitude of the long wavelength modes which initially excite these waves (i.e., via a two-step process). And finally, it has recently been shown that low frequency density fluctuations due to drift waves can stabilize the collisionless, high frequency drift-cyclotron instability (Hasegawa, 1978). Because of similar physical effects, this stabilization mechanism may also stabilize the lower-hybrid-drift instability and therefore, put a nonlinear threshold requirement on the instability. Unfortunately, Hasegawa's stabilization criterion is not applicable for plasma conditions in equatorial Spread F where collisional effects can be important. Furthermore, the magnitude of the low frequency density fluctuations observed in the ionosphere are not well known. However, this stabilization process may indeed be important for equatorial Spread F and a detailed analysis of this effect will be presented later.

Acknowledgement

This work was supported by the Defense Nuclear Agency and the Office of Naval Research. We wish to thank Dr. Bob Goldman for pointing out the importance of ion-ion collisions and Dr. Tom Gladd for helpful discussions.

References

Allan, W., and J. J.Sanderson, Collisional Destruction of the Bernstein Modes in the High Frequency Regime, J. Plasma Phys. 15, 41, 1976.

Costa, E., and M. C. Kelley, On the Role of Steepened Structures and Drift Waves in Equatorial Spread F, J. Geophys. Res. (submitted 1978a).

Costa, E., and M. C. Kelley, Linear Theory for the Collisionless Drift Wave Instability with Wavelengths near the Ion Gyroradius, J. Geophys. Res. (submitted 1978b).

Davidson, R. C., N. T. Gladd, C. S. Wu, and J. D. Huba, Effects of Finite Plasma Beta on the Lower-Hybrid-Drift Instability, Phys. Fluids, 20, 301, 1977.

Dougherty, J. P., Model Fokker-Planck Equation for a Plasma and its Solution, Phys. Fluids, 7, 1788, 1964.

Farley, D. T., B. B. Balsley, R. F. Woodman, and J. P. McClure Equatorial Spread F: Implications of VHF Radar Observations, J. Geophys. Res., 75, 7199, 1970.

Freidberg, J. P., and R. A. Gerwin, Lower Hybrid Drift Instability at Low Drift Velocities, Phys. Fluids, 20, 1311, 1977.

Gary, S. P., and J. J. Sanderson, Density Gradient Drift Instabilities: Oblique Propagation at Zero Beta, Phys. Fluids, (submitted Sept. 1977).

Gladd, N. T., The Lower Hybrid Drift Instability and the Modified Two Stream Instability in High Density Theta Pinch Environments, Plasma Phys., 18, 27, 1976.

Haerendel, G., Theory of Equatorial Spread F, preprint, Max-Planck

Institute fur Physik und Astrophysik, 1974.

Hasegawa, A., Stabilization of Drift-Cyclotron Loss-Cone Mode by Low-Frequency Density Fluctuations, Phys. Rev. Lett., 40, 938, 1978.

Hudson, M. K., C. F. Kennel, and P. K. Kaw, A Two-Step Drift Mode Theory of Equatorial Spread F, Trans. Am. Geophys. Un., 54, 1147, 1973.

Kadomtsev, B. B., Plasma Turbulence, pg. 101, Academic Press, New York, 1965.

Kelley, M. C., G. Haerendel, H. Kappler, A. Valenzuela, B. B. Balsley, D. A. Carter, W. L. Ecklund, C. W. Carlson, B. Hausler, and R. Torbert, Evidence for a Rayleigh-Taylor Type Instability and Upwelling of Depleted Density Regions During Equatorial Spread F, Geophys. Res. Letts., 3, 448, 1976.

Krall, N. A. and P. C. Liewer, Low Frequency Instabilities in Magnetic Pulses, Phys. Rev., A4, 2094, 1971.

McClure, J. P., W. B. Hanson, and J. H. Hoffman, Plasma Bubbles and Irregularities in the Equatorial Ionosphere, J. Geophys. Res., 82, 2650, 1977.

Mikhailovskii, A. B. and A. V. Timofeev, Theory of Cyclotron Instability in a Non-Uniform Plasma, Sov. Phys. JETP, 17, 626, 1963.

Ossakow, S. L., S. T. Zalesak, B. E. McDonald, and P. K. Chaturvedi, Nonlinear Equatorial Spread F: Dependence on Altitude of the F Peak and Bottomside Background Electron Density Gradient Scale Length, J. Geophys. Res., (submitted 1978).

Woodman, R. F., and C. La Hoz, Radar Observations of F-Region Equatorial Irregularities, J. Geophys. Res., 81, 5447, 1976.

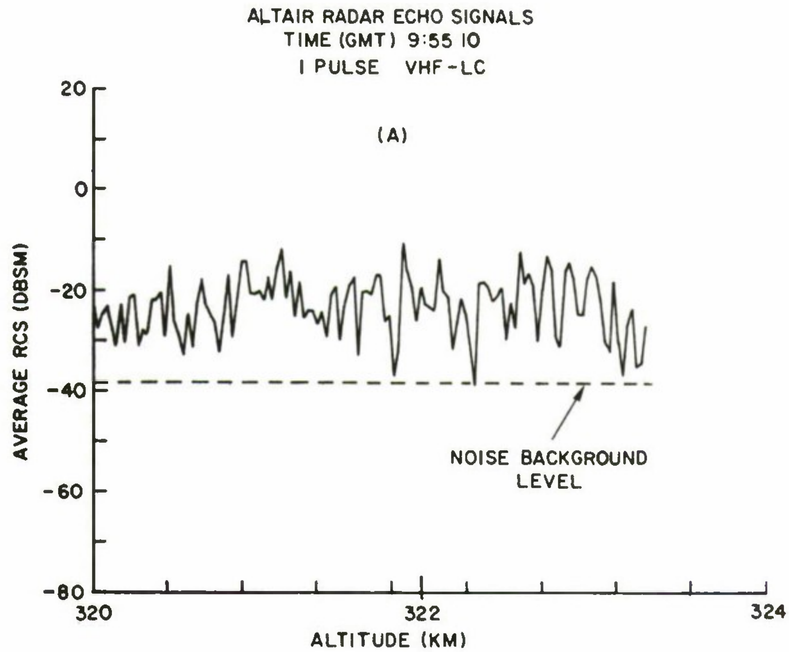
ALTAIR RADAR ECHO SIGNALS
TIME (GMT) 9:55 10
I PULSE VHF-LC
(A)
20
0
-20
-40
-60
-80
AVERAGE RCS (DBSM)
NOISE BACKGROUND LEVEL
320
322
324
ALTITUDE (KM)

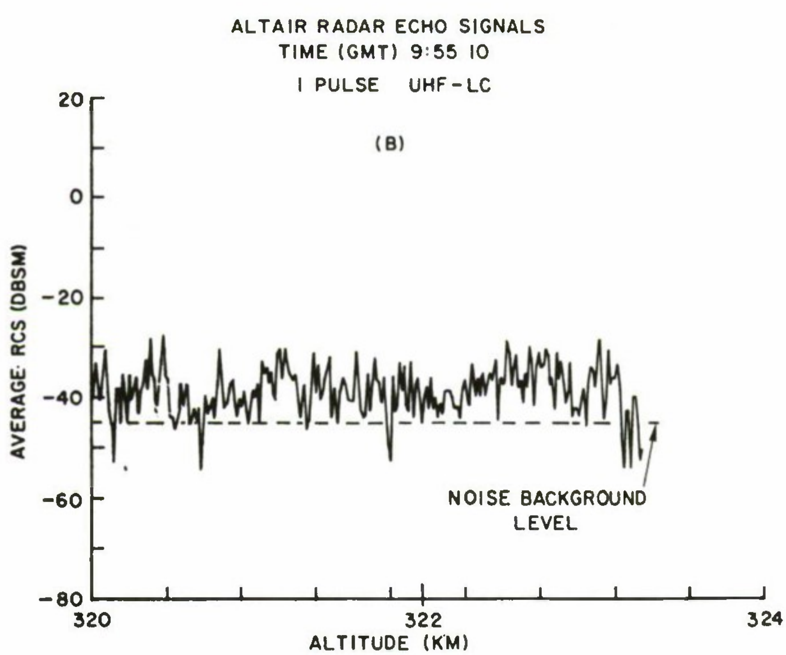
ALTAIR RADAR ECHO SIGNALS
TIME (GMT) 9:55 10
I PULSE UHF-LC
(B)
20
0
-20
-40
-60
-80
AVERAGE RCS (DBSM)
NOISE BACKGROUND LEVEL
320
322
324
ALTITUDE (KM)

Fig. 1 — ALTAIR radar (at Kwajalein) unaveraged received signal (in dB relative to a one m^2 point target) versus altitude for (A) VHF, 155 MHz, and (B) UHF, 415 MHz, for a single pulse at 0955 GMT (2155 LT) on 17 Aug 1977. The radar is observing perpendicular to the magnetic field and sampling the F region starting at 320 km. For (A) there are 124 samples separated by 30m range increments and for (B) there are 246 samples separated by 15m range increments. Both results are from the #1 (of 21) beam scan position with an elevation angle = 65.5° and azimuth angle = −61.0° and with a stationary range recording window. The dashed lines represent the rms noise background. Note that the noise background of the UHF signal, in addition to the total signal strength, is smaller than at VHF. The UHF beam is 1.1° wide while the VHF beam is 2.8° wide.

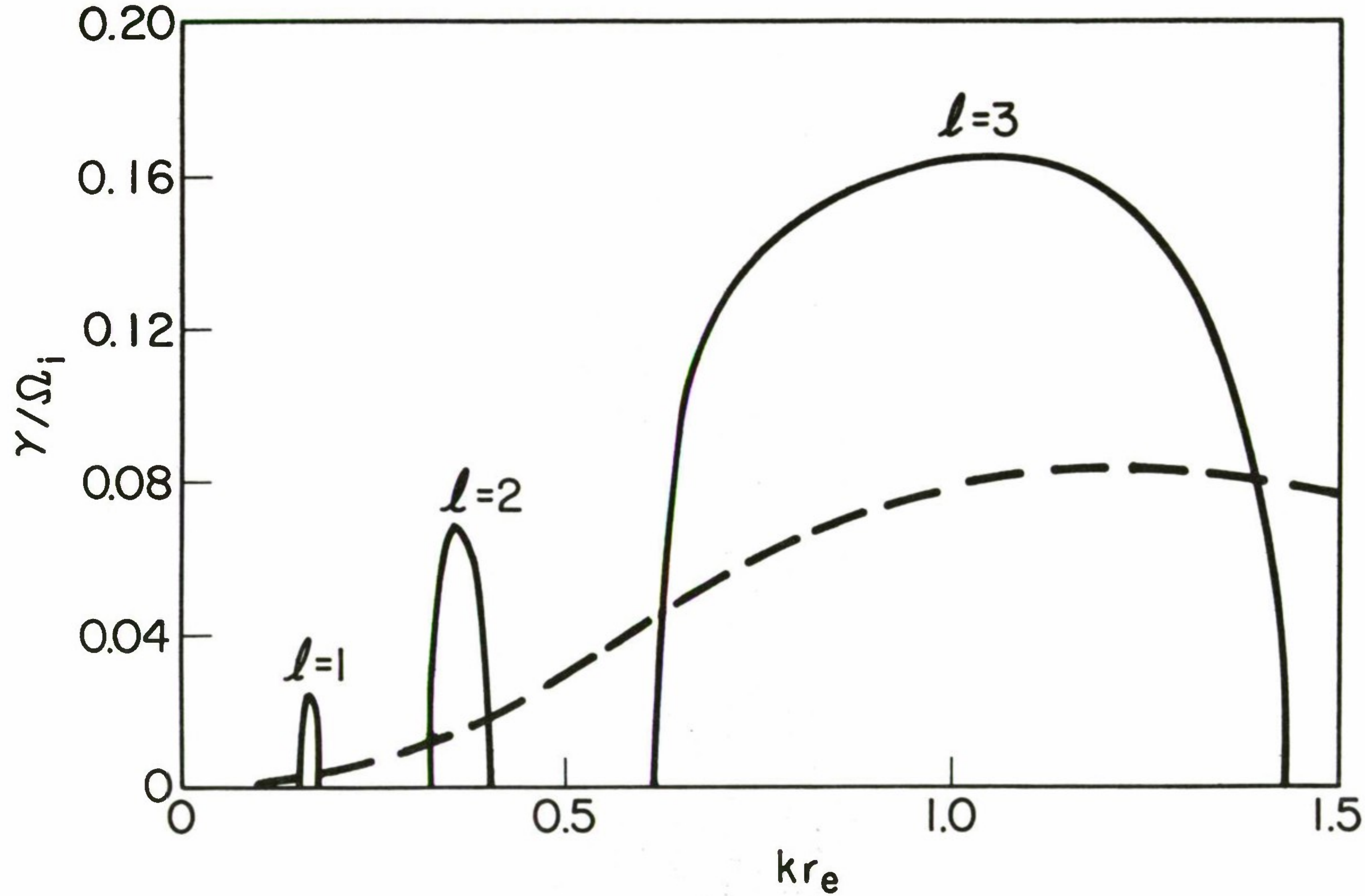

Fig. 2 — Growth rate as a function of perpendicular wavenumber for the DC instability (solid line) and LHD instability (dashed line) for an 0^+ plasma with $T_e = T_i$, $\omega_{pe}/\Omega_e = 10$, and $V_{di}/V_i = 0.037$. Growth also occurs for $kr_e > 1.5$ but has not been plotted.

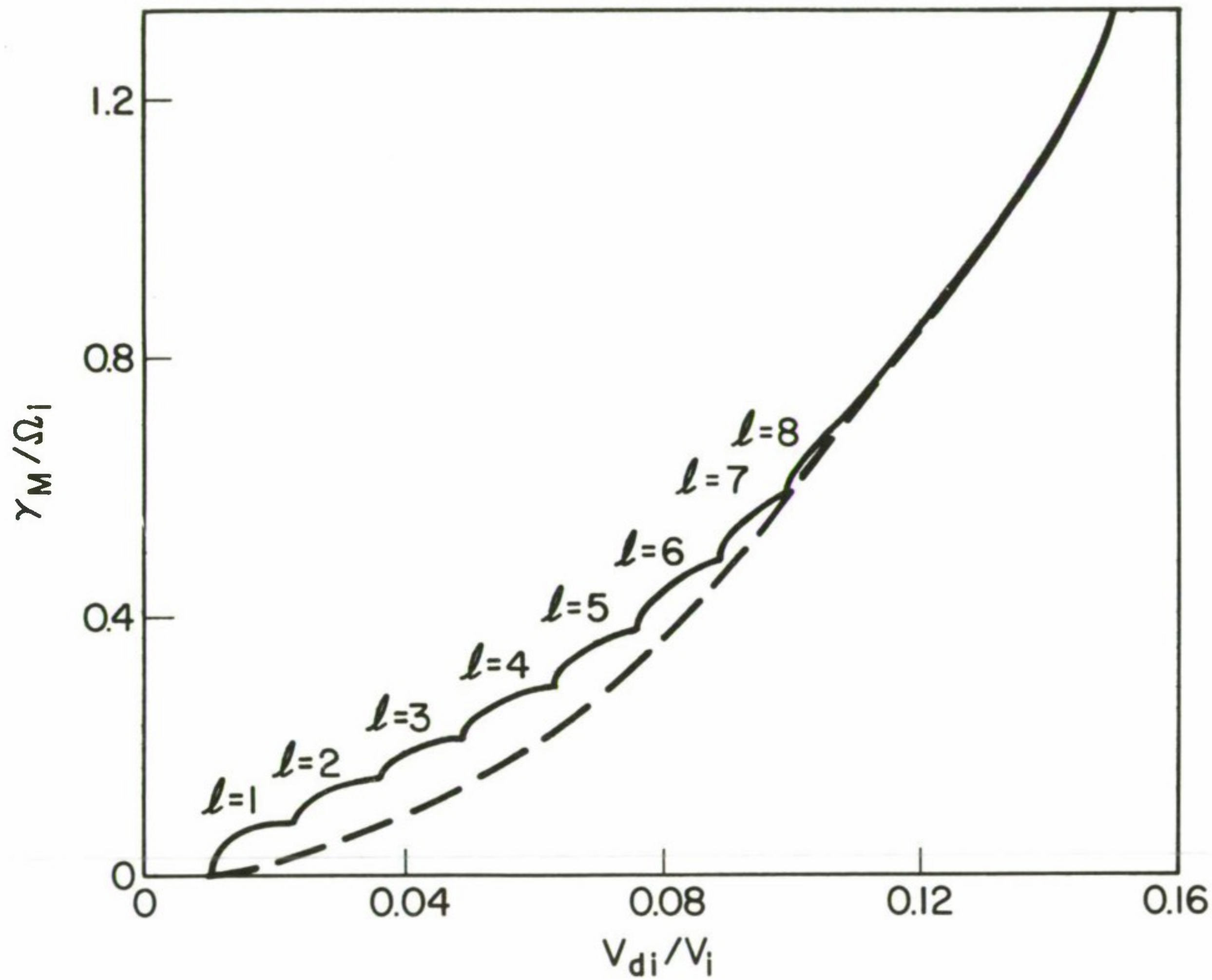

Fig. 3 — Maximum growth rate as a function of ion diamagnetic drift velocity for the DC instability (solid line) and the LHD instability (dashed line). The other parameters are the same as in Fig. 2. Note that the DC instability goes into the LHD instability for $V_{di}/V_i \gtrsim 0.11$.

DISTRIBUTION LIST

DIRECTOR
Defense Advanced Rsch Proj Agency
Architect Building
1400 Wilson Blvd.
Arlington, Va. 22209
ATTN: Strategic Tech Office

Defense Communication Engineer Center
1860 Wiehle Avenue
Reston, Va. 22090
ATTN: CODE R820 R. L. Crawford
ATTN: Code R410 W. D. Dehart

DIRECTOR
Defense Communications Agency
Washington, D. C. 20305
ATTN: CODE 960
ATTN: CODE 480

Defense Documentation Center
Cameron Station
Alexandria, Va. 22314 — 12 copies (if open publication)
ATTN: TC — 2 copies (if otherwise)

DIRECTOR
Defense Intelligence Agency
Washington, D. C. 20301
ATTN: W. Wittig DC - 7D
ATTN: DT-1B

DIRECTOR
Defense Nuclear Agency
Washington, D. C. 20305
ATTN: STSI Archives
ATTN: STVL
ATTN: STTL Tech Library — 2 copies
ATTN: DDST
ATTN: RAAE

DIR OF DEFENSE RSCH & ENGINEERING
Washington, D. C. 20301
ATTN: DD/S&SS John B. Walsh
ATTN: OAD/EPS

COMMANDER
Field Command
Defense Nuclear Agency
Kirtland AFB, NM 87115
ATTN: FCPR
ATTN FCPR COL. John P. Hill
Interservice Nuclear Weapons School
Kirtland AFB, NM 87115
ATTN: Document Control

DIRECTOR
Joint Strat TGT Planning Staff Jcs
Offutt AFB
Omaha, NB 68113
ATTN: JLTW-2
ATTN: JPST G. D. Burton
ATTN: JPST MAJ. J. S. Green

CHIEF
Livermore Division Fld Command DNA
Lawrence Livermore Laboratory
P. O. Box 808
Livermore, CA 94550
ATTN: FCPRL

COMMANDER
National Military Comd Sys Support Ctr
Pentagon
Washington, D. C. 20301
ATTN: B211
ATTN: DP DIRECTOR FOR CSPO

DIRECTOR
National Security Agency
Ft. George G. Meade, Md. 20755
ATTN: W14 Pat Clark
ATTN: Frank Leonard

OJCS/J-3
The Pentagon
Washington, D. C. 20301
ATTN: J-3 OPS ANAL BR. COL. Longsberry

OJCS/J-6
The Pentagon
Washington, D. C. 20301
ATTN: J-6

DIRECTOR
Telecommunications & Comd & Con Sys
Washington, D. C. 20301
ATTN: ASST DIR Info & Space Sys
ATTN: DEP ASST. SEC Sys

Weapons Systems Evaluation Group
400 Army-Navy Drive
Arlington, Va. 22202
ATTN: DOCUMENT CONTROL

COMMANDER
Harry Diamond Laboratories
2800 Powder Mill Road
Adelphi, Md. 20783
ATTN: AMXDO-NP

COMMANDER
TRASANA
White Sands Missile Range, NM 88002
ATTN: EAB

DIRECTOR
U. S. Army Ballistic Research Labs
Aberdeen Proving Ground, Md. 21003
ATTN: AM-CA Franklin E. Niles

U. S. Army Communications CMD
C-B Services Division
Pentagon Rm. 2D513
Washington, D. C. 20310
ATTN: CEAD

COMMANDER
U. S. Army Electronics Command
Fort Mommouth, N. J. 07703
ATTN: AMSEL-TL-ENV Hans A. Bomke

COMMANDER
U. S. Army Material Command
5001 Eisenhower Avenue
Alexandria, Va. 22333
ATTN: AMCRD-WN-RE John F. Corrigan

COMMANDER
U. S. Army Material Command
Foreign and Scientific Tech Center
220 7th St. N. E.
Charlottesville, Va. 22901
ATTN: P. A. Crowley
ATTN: R. Jones

COMMANDER
U. S. Army Missile Command
Redstone Arsenal
Huntsville, Al. 35809
ATTN: AMSMI-YTT W. G. Preussel, Jr.

COMMANDER
U. S. Army Nuclear Agency
Fort Bliss, Tx. 79916
ATTN: USANUA-W. J. Berbert
ATTN: CDINS-E

CHIEF of Naval Research
Department of the Navy
Arlington, Ba. 22217
ATTN: CODE 464 Jacob L. Warner
ATTN: CODE 464 Thomas P. Quinn

COMMANDER
Naval Air Systems Command
Headquarters
Washington, D. C. 21360
ATTN: AIR 5381

COMMANDER
Naval Electronics Systems Command
Naval Electronic System CMD HQS
Washington, D. C. 20360
ATTN: NAVALEX 034 T. Barry Hughes
ATTN: PME 106-1 Satellite Comm Project Off
ATTN: John E. Doncarlos
ATTN: PME 117

COMMANDER
Naval Electronics Laboratory Center
San Diego, CA 92152
ATTN: William F. Moler
ATTN: CODE 2200 Verne E. Hildebrand
ATTN: R. Eastman

COMMANDING OFFICER
Naval Intelligence Support CTR
1301 Suitland Road, Bldg. 5
Washington, D. C. 20390
ATTN: Mr. Dubbin Stic 12

DIRECTOR
Naval Research Laboratory
Washington, D. C. 20375
ATTN: HDQ COMM DIR Bruce Wald
ATTN: CODE 5460 Radio Propagation BR
ATTN: CODE 6701 Jack D. Brown
ATTN: CODE 6700 Division Superintendent — 25 copies (if unclass) / 1 copy (if classified)
ATTN: CODE 6750 Branch Head — 150 copies (if unclass) / 1 copy (if classified)
ATTN: CODE 7127, Chas. Y. Johnson

COMMANDING OFFICER
Naval Space Surveillance System
Dahlgren, Va. 22448
ATTN: CAPT. J. H. Burton

COMMANDER
Naval Surface Weapons Center
White Oak, Silver Spring, Md. 20910
ATTN: CODE 1224 Navy Nuc Prgms Off
ATTN: CODE 730 Tech. Lib.

DIRECTOR
Strategic Systems Project Office
Navy Department
Washington, D. C. 20376
ATTN: NSP-2141

COMMANDER
ADC/AD
ENT AFB, Co., 80912
ATTN: ADDA

Headquarters
U. S. Army Elect Warfare Lab (ECOM)
White Sands Missile Range, NM 88002
ATTN: E. Butterfield

AF Cambridge Rsch Labs, AFSC
L. G. Hanscom Field
Bedford, Ma 01730
ATTN: LKB Kenneth S. W. Champion
ATTN: OPR James C. Ulwick
ATTN: OPR Hervey P. Gauvin

AF Weapons Laboratory, AFSC
Kirtland AFB, NM 87117
ATTN: John M. Kamm SAS
ATTN: SUL
ATTN: DYT LT Mark A. Fry
ATTN: DYT CAPT Wittwer
ATTN: DYT CAPT Gary Cable

AFTAC
Patrick AFB, Fl. 32925
ATTN: TF MAJ. E. Hines
ATTN: TF/CAPT. Wiley
ATTN: TN

Air Force Avionics Laboratory, AFSC
Wright-Patterson AFB, Oh. 45433
ATTN: AFAL AVWE Wade T. Hunt

Assistant Chief of Staff
Studies and Analysis
Headquarters, U. S. Air Force
Washington, D. C. 20330

Headquarters
Electronics Systems Division (AFSC)
L. G. Hanscom Field
Bedford, Ma. 01730
ATTN: XRE LT. Michaels
ATTN: LTC J. Morin CDEF XRC
ATTN: YSEV

COMMANDER
Foreign Technology Division, AFSC
Wright-Patterson AFB, Oh. 45433
ATTN: TD-BTA LIBRARY

HQ USAF/RD
Washington, D. C. 20330
ATTN: RDQ

COMMANDER
Rome Air Development Center, AFSC
Griffith AFB, N. Y. 13440
ATTN: EMTLD Doc Library

COMMANDER IN CHIEF
Strategic Air Command
Offutt AFB, NB 68113
ATTN: XPFS MAJ. Brian G. Stephan

544IES
Offutt AFB, NB 68113
ATTN: RDPO LT. Alan B. Merrill

Los Alamos Scientific Laboratory
P. O. Box 1663
Los Alamos, NM 87544
ATTN: DOC CON for R. F. Taschek
ATTN: DOC CON for Milton Peek
ATTN: DOC CON for Eric Lindman

Sandia Laboratories
P. O. Box 5800
Albuquerque, NM 87115
ATTN: DOC CON for A. Dean Thronbrough
ATTN: DOC CON for W. D. Brown
ATTN: DOC CON for D. A. Dahlgren, ORG 1722
ATTN: DOC CON for J. P. Martin, ORG 1732

University of California
Lawrence Livermore Laboratory
P. O. Box 808
Livermore, CA 94550
ATTN: Tech Info Dept L-3

Department of Commerce
National Oceanic & Atmospheric Admin.
Environmental Research Laboratories
Boulder, CO 80302
ATTN: Joseph H. Pope
ATTN: C. L. Rufenach

Department of Commerce
Office for Telecommunications
Institute for Telecom Science
Boulder, CO 80302
ATTN: Glenn Falcon
ATTN: G. Reed
ATTN: L. A. Berry
ATTN: William F. Utlaut

Department of Transportation
Transportation Rsch. System Center
Kendall Square
Cambridge, MA 02142
ATTN: TER G. Harowles

NASA
Goddard Space Flight Center
Greenbelt, Md 20771
ATTN: CODE 750 T. Golden

NASA
600 Independence Ave., S. W.
Washington, D. C. 20346
ATTN: M. Dubin

Aerodyne Research, Inc.
Tech/Ops Building
20 South Avenue
Burlington, MA 01803
ATTN: M. Camac
ATTN: F. Bien

Aerospace Corporation
P. O. Box 92957
Los Angeles, CA 90009
ATTN: T. M. Salmi
ATTN: S. P. Bower
ATTN: V. Josephson
ATTN: SMFA for PWW
ATTN: R. Grove
ATTN: R. D. Rawcliffe
ATTN: T. Taylor
ATTN: Harris Mayer
ATTN: D. C. Cartwright

Analytical Systems Corporation
25 Ray Avenue
Burlington, MA 01803
ATTN: Radio Sciences

Avco-Everett Research Laboratory, Inc.
2385 Revere Beach Parkway
Everett, MA 02149
ATTN: Richard M. Patrick

Boeing Company, The
P. O. Box 3707
Seattle, WA 98124
ATTN: D. Murray
ATTN: Glen Keister

Brown Engineering Company, Inc.
Cummings Research Park
Huntsville, AL 35807
ATTN: David Lambert MS 18

California at San Diego, Univ. of
Building 500 Mather Campus
3172 Miramar Road
La Jolla, CA 92037
ATTN: Henry G. Booker

Calspan
P. O. Box 235
Buffalo, N. Y. 14221
ATTN: Romeo A. Deliberis

Computer Sciences Corporation
P. O. Box 530
6565 Arlington Blvd.
Falls Church, VA 22046
ATTN: H. Blank
ATTN: Barbara F. Adams

Comsat Laboratories
P. O. Box 115
Clarksburg, Md. 20734
ATTN: R. R. Taur

Cornell University
Department of Electrical Engineering
Ithaca, N. Y. 14850
ATTN: D. T. Farley, Jr.

ESL, Inc.
495 Java Drive
Sunnyvale, CA 93102
ATTN: J. Roberts
ATTN: V. L. Mower
ATTN: James Marshall
ATTN: R. K. Stevens

General Electric Company
Tempo-Center for Advanced Studies
816 State Street
Santa Barbara, CA 93102
ATTN: Don Chandler
ATTN: DASIAC
ATTN: Tim Stephens

General Electric Company
P. O. Box 1122
Syracuse, N. Y. 13201
ATTN: F. A. Reibert

General Research Corporation
P. O. Box 3587
Santa Barbara, CA 93105
ATTN: John Ise, Jr.

Geophysical Institute
University of Alaska
Fairbanks, AK 99701
ATTN: Technical Library
ATTN: Neil Brown
ATTN: T. N. Davis

GTE Sylvania, Inc.
189 B Street
Needham Heights, MA 02194
ATTN: Marshall Cross

HRB-SINGER, Inc.
Science Park, Science Park Road
P. O. Box 60
State College, PA 16801
ATTN: Larry Feathers

Honeywell Incorporated
Radiation Center
2 Forbes Road
Lexington, MA 02173
ATTN: W. Williamson

Illinois, University of
Department of Electrical Engineering
Urbana, IL 61801
ATTN: K. C. Yeh

Institute for Defense Analyses
400 Army-Navy Drive
Arlington, VA 22202
ATTN: Ernest Bauer
ATTN: Hans Wolfhard
ATTN: J. M. Aein
ATTN: Joel Bengston

Intl Tel & Telegraph Corporation
500 Washington Avenue
Nutley, N. J. 07110
ATTN: Technical Library

ITT Electro-Physics Laboratories, Inc.
9140 Old Annapolis Road
Columbus, Md. 21043
ATTN: John M. Kelso

Johns Hopkins University
Applied Physics Laboratory
8621 Georgia Avenue
Silver Spring, MD 20910
ATTN: Document Librarian

Lockheed Missiles & Space Co., Inc.
P. O. Box 504
Sunnyvale, CA 94088
ATTN: Dept. 60-12

Lockheed Missiles and Space Company
3251 Hanover Street
Palo Alto, CA 94304
ATTN: Billy M. McCormac, Dept 52-14
ATTN: Martin Walt, Dept 52-10
ATTN: Richard G. Johnson, Dept 52-12
ATTN: JOHN CLADIS

MIT Lincoln Laboratory
P. O. Box 73
Lexington, MA 02173
ATTN: Mr. Walden, X113
ATTN: D. Clark
ATTN: James H. Pannell, L-246
ATTN: Lib A-082 for David M. Towle

Martin Marietta Corporation
Denver Distribution
P. O. Box 179
Denver, CO 80201
ATTN: Special Projects Program 248

Maxwell Laboratories, Inc.
9244 Balboa Avenue
San Diego, CA 92123
ATTN: A. J. Shannon
ATTN: V. Fargo
ATTN: A. N. Rostocker

McDonnell Douglas Corporation
5301 Bolsa Avenue
Huntington Beach, CA 92657
ATTN: J. Moule
ATTN: N. Harris

Mission Research Corporation
735 State Street
Santa Barbara, CA 93101
ATTN: R. Hendrick
ATTN: Conrad L. Longmire
ATTN: Ralph Kilb
ATTN: R. E. Rosenthal
ATTN: R. Bogusch
ATTN: David Sowle
ATTN: M. Scheibe
ATTN: P. Fischer

Mitre Corporation, The
Route 62 and Middlesex Turnpike
P. O. Box 208
Bedford, MA 01730
ATTN: Chief Scientist W. Sen
ATTN: S. A. Morin M/S
ATTN: C. Harding

North Carolina State Univ At Raleigh
Raleigh, N. C. 27507
ATTN: SEC Officer for Walter A. Flood

Pacific-Sierra Research Corp.
1456 Cloverfield Blvd.
Santa Monica, CA 90404
ATTN: E. C. Field, Jr.

Philco-Ford Corporation
Western Development Laboratories Div
3939 Fabian Way
Palo Alto, CA 94303
ATTN: J. T. Mattingley MS X22

Photometrics, Inc.
442 Marrett Road
Lexington, MA 02173
ATTN: Irving J. Kofsky

Mitre Corporation, The
Westgate Research Park
1820 Dolley Madison Blvd.
McLean, VA 22101
ATTN: Allen Schneider

Physical Dynamics, Inc.
P. O. Box 1069
Berkeley, CA 94701
ATTN: Joseph B. Workman

Physical Sciences, Inc.
607 North Avenue, Door 18
Wakefield, MA 01880
ATTN: Kurt Wray

R & D Associates
P. O. Box 3580
Santa Monica, CA 90403
ATTN: Robert E. Lelevier
ATTN: Forest Gilmore
ATTN: Richard Latter
ATTN: William B. Wright, Jr.

R & D Associates
1815 N. Ft. Myer Drive
11th Floor
Arlington, VA 2209
ATTN: Herbert J. Mitchell

Rand Corporation, The
1700 Main Street
Santa Monica, CA 90406
ATTN: Cullen Crain

Science Applications, Inc.
P. O. Box 2351
La Jolla, CA 92038
ATTN: Daniel A. Hamlin
ATTN: D. Sachs
ATTN: E. A. Straker

Space Data Corporation
1331 South 26th Street
Phoenix, AZ 85034
ATTN: Edward F. Allen

Stanford Research Institute
333 Ravenswood Avenue
Menlo Park, CA 94025
ATTN: M. Baron
ATTN: L. L. Cobb
ATTN: Walter G. Chestnut
ATTN: David A. Johnson
ATTN: Charles L. Rino
ATTN: E. J. Fremouw
ATTN: Ray L. Leadabrand
ATTN: Donald Neilson

Stanford Research Institute
306 Wynn Drive, N. W.
Huntsville, AL 35805
ATTN: Dale H. Davis

Technology International Corporation
75 Wiggins Avenue
Bedford, MA 01730
ATTN: W. P. Boquist

TRW Systems Group
One Space Park
Redondo Beach, CA 90278
ATTN: P. H. Katsos
ATTN: J. W. Lowery

Utah State University
Contract/Grant Office
Logan, UT 84322
ATTN: Security Officer

Visidyne, Inc.
19 Third Avenue
North West Industrial Park
Burlington, MA 01803
ATTN: William Reidy
ATTN: Oscar Manley
ATTN: J. W. Carpenter

Please distribute one copy to each of the following people:

Advanced Research Projects Agency (ARPA)
Strategic Technology Office
Arlington, Virginia

Capt. Donald M. LeVine

Naval Research Laboratory
Washington, D.C. 20375

Dr. P. Mange
Dr. E. Peterkin
Dr. R. Meier
Dr. E. Szuszczewicz - Code 7127

Science Applications, Inc.
1250 Prospect Plaza
La Jolla, California 92037

Dr. D. A. Hamlin
Dr. L. Linson
Dr. D. Sachs

Director of Space and Environmental Laboratory
NOAA
Boulder, Colorado 80302

Dr. A. Glenn Jean
Dr. G. W. Adams
Dr. D. N. Anderson
Dr. K. Davies
Dr. R. F. Donnelly

A. F. Cambridge Research Laboratories
L. G. Hanscom Field
Bedford, Mass. 01730

Dr. T. Elkins
Dr. W. Swider
Mrs. R. Sagalyn
Dr. J. M. Forbes
Dr. T. J. Keneshea
Dr. J. Aarons

Office of Naval Research
800 North Quincy Street
Arlington, Virginia 22217

Dr. J. G. Dardis
Dr. H. Mullaney

Commander
Naval Electronics Laboratory Center
San Diego, California 92152

Dr. M. Bleiweiss
Dr. I. Rothmuller
Dr. V. Hildebrand
Mr. R. Rose

U. S. Army Aberdeen Research and Development Center
Ballastic Research Laboratory
Aberdeen, Maryland

Dr. F. Niles
Dr. J. Heimerl

Commander
Naval Air Systems Command
Department of the Navy
Washington, D.C. 20360

Dr. T. Czuba

Harvard University
Harvard Square
Cambridge, Mass. 02138

Dr. M. B. McElroy
Dr. R. Lindzen

Pennsylvania State University
University Park, Pennsylvania 16802

Dr. J. S. Nisbet
Dr. P. R. Rohrbaugh
Dr. D. E. Baran
Dr. L. A. Carpenter
Dr. M. Lee
Dr. R. Divany
Dr. P. Bennett
Dr. E. Klevans

University of California, Los Angeles
405 Hillgard Avenue
La Jolla, California 90024

Dr. F. V. Coroniti
Dr. C. Kennel

University of California, Berkeley
Berkeley, California 94720

Dr. M. Hudson

Utah State University
4th N. and 8th Streets
Logan, Utah 84322

Dr. P. M. Banks
Dr. R. Harris
Dr. V. Peterson
Dr. R. Megill

Cornell University
Ithaca, New York 14850

Dr. W. E. Swartz
Dr. R. Sudan
Dr. D. Farley
Dr. M. Kelley
Dr. E. Ott

NASA
Goddard Space Flight Center
Greenbelt, Maryland 20771

Dr. S. Chandra
Dr. K. Maedo

Princeton University
Plasma Physics Laboratory
Princeton, New Jersey 08540

Dr. F. Perkins

Institute for Defense Analysis
400 Army/Navy Drive
Arlington, Virginia 22202

Dr. E. Bauer